NUMERICAL SIMULATION OF DECAY HEAT SCATTERING OUT OF AP1000 NUCLEAR REACTOR SPENT FUEL CASK BASED ON FINITE ELEMENT METHOD

by

Shujian TIAN[a*], Guozhuang LI[b], Jun LIU[a], Haoyun YUAN[a], Xiaoyong SONG[a], and Weishu WANG[a]

[a]School of Electric Power, North China University of Water Resources and Electric Power, Zhengzhou, Henan, China
[b]School of Nuclear Science and Technology, University of South China, Hengyang, Hunan, China

Original scientific paper
https://doi.org/10.2298/TSCI191023011T

The heat transfer performance of the spent fuel transport cask is inseparably related to the safety of the whole reprocessing system. In this study, we carried out the thermal analysis on the NAC-STC transport cask for AP1000 spent fuel assembly to evaluate the thermal performance of transport cask by the finite element method software ANSYS. A computational dynamics model was developed to study the temperature distribution inside the transport cask and on the surface of the cask. The effectiveness of the numerical calculation is demonstrated by comparing with the theoretical results. The results show that transport cask can reach steady-state during transportation, and the highest temperature in the case is 328 ℃, which is below the maximum safety limit of 400 ℃. Besides, the temperature of the fuel element baskets, sealing ring, photon shielding layer and neutron shielding layer in the cask are all within the safety limit.

Keywords: *NAC-STC transport cask, AP1000 spent fuel assembly, thermal analysis, temperature distribution*

Introduction

Since the AP1000 unit of Sanmen Nuclear Power Plant was built and put into operation, the operation of the units is safe and stable, and all the technical indexes are in accordance with safety regulations. However, in order to ensure the long-term safe operation of nuclear power plants, the spent fuel discharged from the reactor after a certain time of cooling must be transported to the reprocessing plant post-processing. The NAC company spent fuel transport cask (NCA-STC) has been widely used to transport spent fuel assemblies of pressurized-water reactor (PWR) in China [1-3]. If the thermal conductivity of the cask is weak, the decay heat of the spent fuel assembly discharged from the reactor core can build up and can eventually cause the vessel to meltdown. Therefore, the performance of the thermal conductivity of the cask in the transport process is vital. At present, the thermal analysis of the second generation advanced fuel assembly (AFA-2G) and the third generation advanced fuel

*Corresponding author, e-mail: tianshujian@ncwu.edu.cn

assembly (AFA-3G) PWR fuel assembly has been studied internationally [4-6]. Wix and Hohnstreiter [7] analyzed and studied the convection coefficient under the premise of ignoring the internal convection. Bullard *et al*. [8] stimulated the heat transmission inside the fuel assembly by using CFD. Frano *et al*. [9] used ANSYS to calculate the temperature distribution under different conditions with ANG-1 type as research model. Most of the selected cask types are NAC-STC transport cask. A comparison of current study results indicates that the NAC-STC cask has better thermal performance, and the research and experimental data are relatively more perfect compared with the General Electric IF-300 shipping cask which is also used for transporting the spent fuel of PWR. Hence, NAC-STC is also the main type of transport cask used in China. However, the internal temperature distribution must be different during transportation when the same type of cask carries different types of spent fuel assemblies. Up to now, no studies have shown that the NAC-STC casks can perform well in the thermal conductivity when transporting AP1000 spent fuel. In addition, most of the research focused on the fuel assembly, aiming to obtain the temperature distribution inside the assembly. The article aims to obtain the temperature distribution of the whole cask. The analysis of the decay heat conducted out of the spent fuel cask should be studied with the steady-state thermal analysis module of ANSYS software.

Based on the existing related data of the transport cask and AP1000 spent fuel assembly, the study on the decay heat conducted out of the spent fuel cask was carried out to obtain the temperature distribution data of the transport cask loading the AP1000 spent fuel assembly. The simulation results in this paper can provide basic data for future study on NAC-STC spent fuel cask.

Research object and analysis method

Fuel assembly parameters

At present, AP1000 has been put into operation in the Sanmen Nuclear Power Plant, which is the introduction and absorption of the third-generation reactors. The fuel assemblies used by the AP1000 are the improved performance fuel assemblies based on AFA-2G, and tab. 1 shows the basic parameters of AP1000 spent fuel assemblies [10-13]. The single assembly weighs 796 kg, and arranged in a 17 × 17 square arrangement, including 264 fuel rods, 24 control rods, and 1 neutron flux rate measuring tube. Furthermore, the designed average burn up is 60 GWd/tU, the fuel enrichment is between 1.6% and 4.5 %, and the refueling cycle is 18 months.

Table 1. Basic parameters of AP1000 spent fuel assemblies [10-13]

Parameter	Numerical value
Single assembly weight [kg]	796
Square arrangement	17 × 17
The design average burn up [$GWdt^{-1}U^{-1}$]	60
The full length of fuel assembly [cm]	479.84
Fuel enrichment [%]	1.6~4.5
Fuel assembly active zone length [cm]	426.72
Fuel assembly padding [cm]	214.5
Refueling cycle [month]	18
Number of normal refueling units per cycle	64

Spent fuel transport cask structure

Figure 1 shows the NAC-STC transport cask structure. The NAC-STC transport cask structure consists of the cask seal system (such as seal end cover, seal rubber ring and bolt), container cylinder, fuel basket (fuel sleeve, heat transfer plate, support plate), shock absorber, and shield and stainless-steel cladding (lead shield, neutron shield). The upper and lower parts of the container cylinder are provided with bolt holes and air holes. The bolt hole is used to fix the upper and lower end caps, and the sealing rubber ring is fixed on the contact surface between the end cover and the barrel body [14]. The fuel basket is used to provide storage space for each spent fuel assembly. Therefore, the spent-fuel sleeve should be designed in accordance with the detailed dimensions of the AP1000 spent fuel assembly and left some space to cope with the fuel assembly thermal expansion and damage due to sleeve compression.

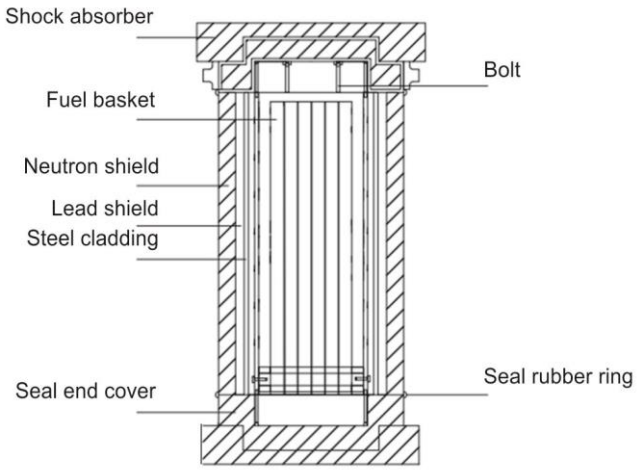

Figure 1. The NAC-STC transport cask structure

The thermal safety analysis method

The primary purpose of thermal safety analysis is to determine whether the thermal conductivity of the NAC-STC cask is good under normal transportation conditions. The ANSYS steady-state thermal analysis is a common software to calculate the temperature distribution on the steady-state thermal condition. The temperature distribution inside the NAC-STC cask during transportation was simulated by the ANSYS steady-state thermal analysis module [15]. Combined with the temperature safety limit of materials used in each part of the cask, the temperature distribution aforementioned is used to evaluate the safety and feasibility of the NAC-STC transport cask loading the AP1000 spent fuel assembly during transportation.

Model establishment and boundary condition determination

Model simplification and heat transfer mechanism

– Since the cask and fuel assembly are on the symmetry of the ZOY and ZOX plane, only a quarter of the geometric model of the cask is established in the calculation model.

- Shock absorbers are not included in the calculation model. As the main structural material of the shock absorbers is wood, and the reduced heat transfer performance of wood, the upper and lower ends of the cask can be set as adiabatic.
- After the homogenization of fuel assemblies, it can be considered that the 32 fuel assembly is a spent fuel assembly with the same enrichment and burn up depth, and their radial and axial thermal conductivity can be calculated accordingly.
- The components such as bolts, welders, and air holes on the outside of the cask shell have little influence on the heat transfer analysis [16]. Therefore, there is no modelling in the modelling process.
- The gap heat transfer model of the gap between fuel assembly and sleeve, the gap between the inner layer of barrel and cladding, and the gap between the lead layer and the outer shell layer is treated equivalently.
- The fuel sleeve is divided into three layers. It can be simplified by means of homogenization of materials [16]. The inner and outer layers are made of 304 stainless steel, and the middle layer is BORAL plate containing boron neutron absorption material. Therefore, the material is homogenized.
- There are 24 NS4FR resins in the neutron shielding layer, and there is a fin between every two resins. Therefore, homogenization is carried out on them.

The spent fuel transport cask is filled with helium gas. Helium gas has a weak flow. Thus, its flow of heat transfer is negligible. In conclusion, the heat transfer mode of the spent fuel transport cask includes the heat conduction of heat transfer plate in fuel basket, the heat conduction of the contact part between the lower barrel body and the end cover, the heat radiation of the gap between the spent fuel assembly and the sleeve, and the solar radiation.

Finite element meshing

Figure 2 shows the result of finite element meshing. Mesh generation was carried out by the mechanical meshing function module in ANSYS workbench. The number of grid nodes is 1723065, the number of grids is 37.0035, and the minimum mesh size is 35 mm. These parameters can meet the requirement of meshing the gap with a small size. The mesh independence of simulation results can be guaranteed under the number of grids.

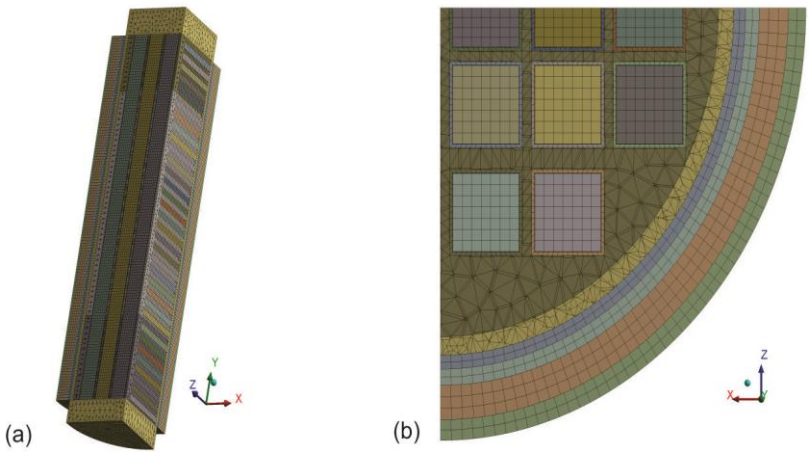

Figure 2. Calculation model and meshing; (a) the results of overall model meshing (b) cross-section of meshing results

The calculation of material property parameter

Homogenization parameters of the spent fuel assemblies

Because of the structural characteristics of spent fuel assemblies, the radial and axial thermal conductivity are different. The AP1000 fuel assembly is similar in structure, although its geometry is different from that of the AFA-2G fuel assembly. According to the 2-D finite element analysis of PWR fuel assembly established by oak ridge laboratory, the axial thermal conductivity of spent fuel assemblies at different temperatures in the helium atmosphere is obtained [17]. Combined with the ambient temperature of the spent fuel assembly at about 300 ℃, the axial thermal conductivity of the spent fuel assembly is approximately set as 1.04 W/(m℃). The main materials in the AP1000 spent fuel assembly are zirconium niobium alloy, carbon steel, boron-containing water, and uranium dioxide. The radial heat conduction coefficient of spent fuel assembly calculated by area weight method is 3.30 W/(m℃). Furthermore, the equivalent density and the equivalent specific heat capacity of spent fuel assemblies are calculated as 3.88 g/cm^3 by the equivalent volume weight method and 1.04 J/(kg℃) at 300 ℃ by mass weighting method, respectively.

Neutron-shield homogenization

The neutron shield is wrapped in stainless steel, and there are 24 NS4FR neutron shielding resins. There is a stainless-steel fin mainly made of 304 stainless steel and copper between each shielding resin. The neutron shield with a complex structure is homogenized. Table 2 shows the equivalent parameters of the neutron shield.

Table 2. Equivalent thermodynamic parameters of neutron shielding

Thermodynamic parameter	Values
Coefficient of thermal conductivity [Wm^{-1}K^{-1}]	8.9041
Density [kgm^{-3}]	1927
Specific heat capacity [Jkg^{-1}℃$^{-1}$)]	1305

Homogenization of fuel sleeve

The fuel sleeve consists of three layers of material. The inner and outer layers are 304 stainless steel and its intermediate layer is the neutron absorbing material BORAL plate. The total thickness of the fuel sleeve is 4 mm. The thickness of the inner stainless-steel layer is 1.20 mm. The thickness of the BORAL plate is 2 mm, and the thickness of the outer stainless steel is 0.80 mm. Equivalent density and equivalent specific heat capacity are analogous to the equivalent parameters of fuel assemblies. Table 3 shows the equivalent thermodynamic parameters of the fuel sleeve.

Table 3. Equivalent thermodynamic parameters of fuel sleeve

Thermodynamic parameter [℃]	36	200
Radial thermal conductivity [Wm^{-1}K^{-1}]	49.21	52.64
Axial thermal conductivity [Wm^{-1}K^{-1}]	50.33	48.20
Density [kgm^{-3}]	5017	
Specific heat capacity [Jkg^{-1}℃$^{-1}$]	612.57	706.31

The treatment of clearance

Interstitial heat transfer includes heat conduction and heat radiation. The gap heat conduction model can be equivalent to a single heat conduction model by calculating the equivalent heat conduction coefficient. Total heat transfer rate of gap heat transfer model can be calculated:

$$\boldsymbol{q} = \boldsymbol{q}_r + \boldsymbol{q}_k \tag{1}$$

where $\boldsymbol{q}_r$ [W] is heat radiation heat transfer rate and $\boldsymbol{q}_k$ [W] is rate of thermal conductivity.

The equivalent emissivity between two parallel planes can be obtained by the following Kreith equation [18]:

$$\varepsilon = \frac{1}{\frac{1}{\varepsilon_1} + \frac{1}{\varepsilon_2} - 1} \tag{2}$$

where ε_1 and ε_2 are two parallel radiation rates.

Table 4 shows the equivalent thermal conductivity of the gap between the fuel assembly and the sleeve. In addition, tab. 5 shows the equivalent thermal conductivity of the gap between the cask barrel and the lead layer.

Table 4. Equivalent thermodynamic parameters of the clearance between fuel and sleeve

Thermodynamic parameter	Temperature [°C]			
	100	200	300	350
Thermal conductivity [$Wm^{-1}K^{-1}$]	0.1731	0.2071	0.2514	0.3046

Table 5. Equivalent thermodynamic parameters of the clearance between cylinder and lead layer.

Thermodynamic parameter	Temperature [°C]			
	100	200	300	350
Thermal conductivity [$Wm^{-1}K^{-1}$]	0.1726	0.2011	0.2354	0.2664

The determine of the calculation model thermal load

Decay heat of spent fuel

The active zone height of the AP1000 spent fuel assembly is 4.1960 m. In this design, the conservative decay heat power of single spent fuel assembly is 1.08 kW [19-21]. Hence, the volume of the produced decay heat can be calculated as 0.21 m^3.

The heat generation rate is calculated as $4.91 \cdot 10^{-6}$ W/mm^2 by:

$$q = \frac{q_d}{32}\frac{1}{v} \tag{3}$$

where q_d is total exothermic rate of the spent fuel (28.08 kW), and v is the volume of the spent fuel.

Solar radiation from the surface of the cask

The solar radiation received by the cask during transportation occurs during the loading and unloading of the cask and in some parts of the cask during transportation. According to the corresponding regulations of the transport cask, the circumferential surface of the cask receives a solar heat load of 193 W/m^2 in one day, and the heat load of upper and lower end surfaces is 388 W/m^2 [19-21]. Equation (4) indicates the calculation of the heat flux generated by sunlight:

$$q_s = \varepsilon J_s \tag{4}$$

Hence, the heat flux density of solar radiation is calculated as $6.979 \cdot 10^{-5}$ W/mm^2.

Convection heat transfer on the surface of the cask

In this study, the selected Baumeister heat transfer model is a cylindrical heat transfer model exposed to air and placed horizontally. The convective heat transfer coefficient of the outer surface is:

$$h_c = 1.3098(T - T_\infty)0.33\left[63.5664D^3(T - T_\infty) \geq 100\right] \tag{5}$$

where D [m] is the diameter of the outer surface of the cask and h_c is the convective heat transfer coefficient on the surface of the cask.

Total heat flux on the outer surface of the transport cask:

$$\begin{gathered} q_T = q_c + q_r - q_s \\ q_T = h_{\text{eff}}(T - T_\infty) \\ h_{\text{eff}} = \sigma F \varepsilon\left[\left(T + 273^2\right) + \left(T_\infty + 273^2\right)\right]\left[(T + 273) + T_\infty + 273\right] + 1.3098(T - T_\infty)0.33 - \frac{J_s}{T - T_\infty} \end{gathered} \tag{6}$$

where $\varepsilon = 0.36$, $\sigma = 5.67 \cdot 10^{-}8$ W/(m^2℃^{4}), and $F = 1$.

There is the convection heat transfer between the surface of the cask and the outside air. The equivalent convective heat transfer coefficient is set as h_{eff} on the outer surface of the model in ANSYS software. The coefficient is a function that varies with the temperature, T, of the cask surface. Therefore, when the convective heat transfer is applied to the outer surface of the cask, the convective heat transfer coefficient is selected as a function varying with temperature, and the applied surface is the outer surface of the neutron shield. The ambient temperature is set as 22 ℃, and the other surface of the cask is set as adiabatic without setting boundary conditions.

Results and discussions

Theoretical calculation and verification

The transport cask keeps in a steady-state heat transfer process when the heat transfer conditions are stable, and the boundary conditions such as heat source, heat power do not change. In steady-state heat transfer, the heat released from the heat source is equal to the heat lost from the cask. Therefore, the heat lost from the cask q_T can be calculated by:

$$q_T = \frac{q_d}{A} \tag{7}$$

where q_T [Wmm^{-2}] is the heat lost from the cask, q_d [W] is the spent fuel thermal power, and A [mm^2] is the spent fuel area.

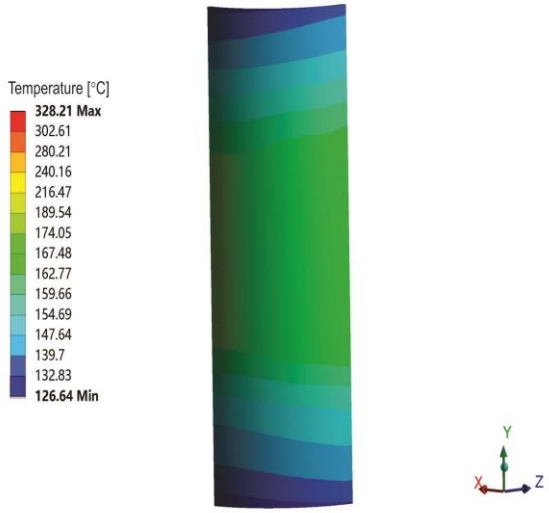

Figure 3. Temperature contours of cask surface

The total area of the outer circumference of the cask is 36 m^2. The equation about temperature, T, is obtained by substituting the area, A, and the spent fuel thermal power, q_d. The outer surface temperature is calculated as 140.68 ℃. Figure 3 shows the temperature distribution of the outer surface obtained by ANSYS simulation. The average surface temperature of the cask is 139.62 ℃, which is close to the theoretical calculation value, indicating the validness of the theoretical model.

Temperature distribution in different parts of the cask

The temperature distribution in different parts of the cask is shown in figs. 4-6. The following conclusions can be obtained from these figures:

- According to fig. 4, the temperature of the spent fuel assembly gradually decreases from the inside out, and the highest temperature is in the innermost fuel assembly. Although the decay heat power of every spent fuel assembly is the same, because of the fuel assembly arrangement, the innermost layer has more heat accumulation, and the outer layer has less.
- The material chosen for the photon shield is the chemical agent lead, whose safe temperature range is –40~316 ℃. Figure 5 shows the temperature distribution of the simulated photon shield. According to fig. 5, the temperature of each part is lower than 316 ℃, which can ensure the normal operation of the photon shielding layer.
- The material of the neutron shielding layer is NS-4-FR shielding resin, and its safe temperature range is –40~149 ℃. The cloud chart of its temperature distribution is shown in fig. 6(a). Figure 6(a) shows that the temperature of each part of the neutron shielding layer is within the safe range, which can ensure the normal operation of the neutron shielding layer.
- The temperature distribution of the position of the O-type sealing ring is shown in fig. 6(b). The highest temperature is 172.35 ℃, which is lower than the allowable temperature of rubber material, 200 ℃. Therefore, the rubber sealing ring can be used.

Radial temperature distribution at different heights

The radial sections at the height of 1 m, 2 m, 3 m, 4 m, and 5 m of the model are selected in this section, and eight position points are selected that are 0 m, 0.2 m, 0.4 m, 0.6 m, 0.8 m, 1.0 m, 1.2 m, and 1.4 m away from the central axis. The authors compartmentalized the radial section into seven sub-sections, namely, sub-sections a, b, c, d, e, f, and g. The corresponding temperature distribution and curves of sections at different heights are shown in figs. 7-11. Sub-sections a, b, and c are the locations of spent fuel assemblies. Thus, the temperatures in sub-sections a, b, and c are all above 200 ℃, and the temperatures gradually decrease from the inside to the outside. Although the decay heat power set is the same, there is heat accumulation in the innermost part due to the arrangement. Sub-sections c and d at the lower temperature are the contact positions between the sleeve and the heat transfer plate or the

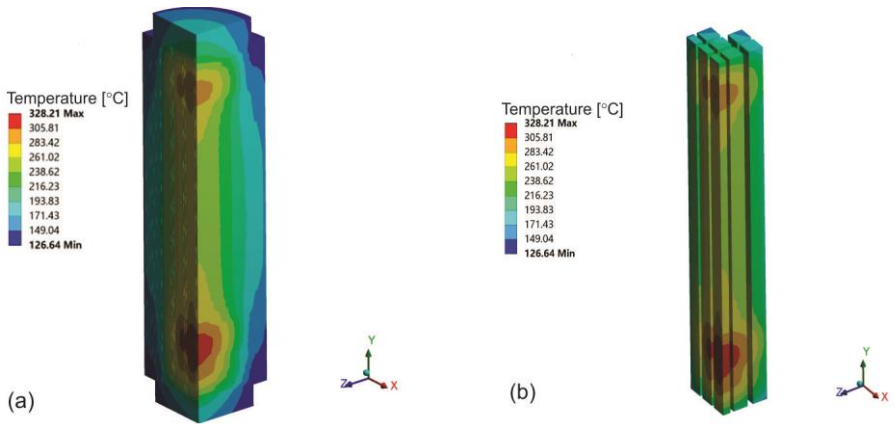

Figure 4. Temperature contours of the whole cask and the spent fuel assemblies; (a) the cask surface (b) the spent fuel assemblies

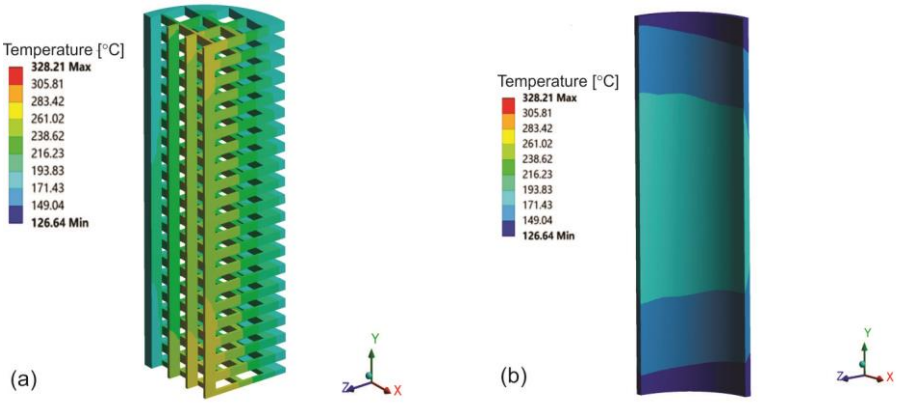

Figure 5. Temperature contours of the heat transfer plate and the lead layer; (a) the heat transfer plate (b) the lead layer

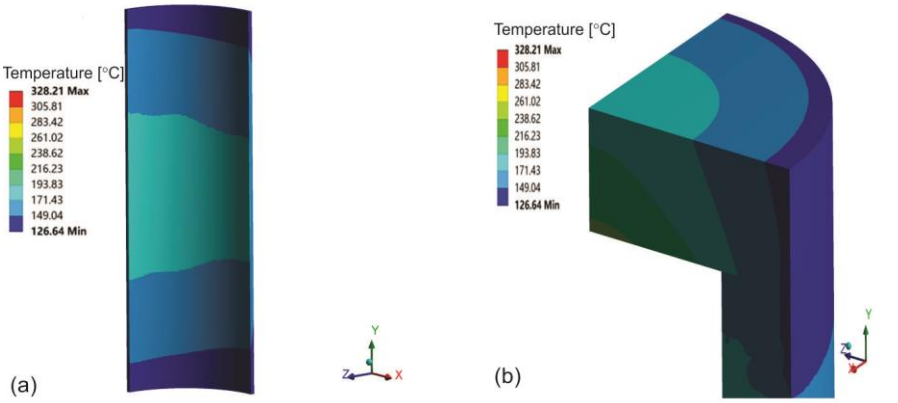

Figure 6. Temperature contours of the neutron shielding and the seal ring; (a) the neutron shielding (b) the seal ring

support plate. The sleeve at the height of 2 m, 3 m, and 4 m is in contact with the heat transfer plate. Because the heat transfer plate is aluminum alloy with better thermal conductivity, the temperature gradient is small. The sleeve is in contact with the support plate at 1 m and 5 m. The support plate is xm-19 stainless steel, which has high strength but relatively poor thermal conductivity. Hence, the support plate has a broader temperature gradient. The areas of f and g are the shielding layer and the stainless-steel outer layer surrounding the cylinder, with thermal conductivity and gap heat exchange. The smaller thermal conductivity coefficient and the weaker heat transfer capacity of the shielding layer also result in the broader temperature gradient.

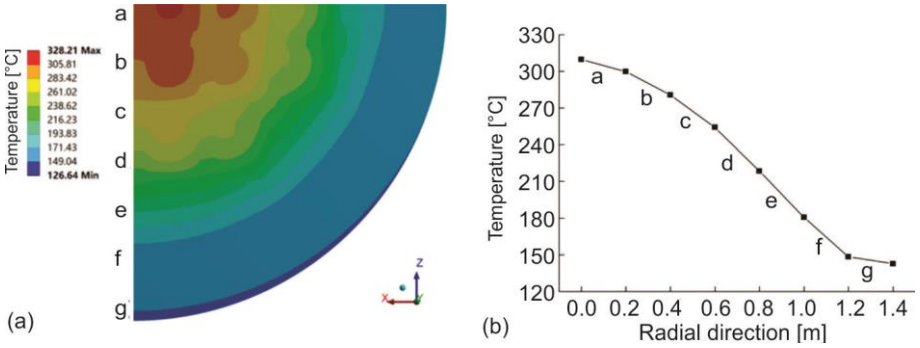

Figure 7. Temperature contours and curve of radial cross section at 1 m height; (a) temperature distribution cloud map (b) temperature curve

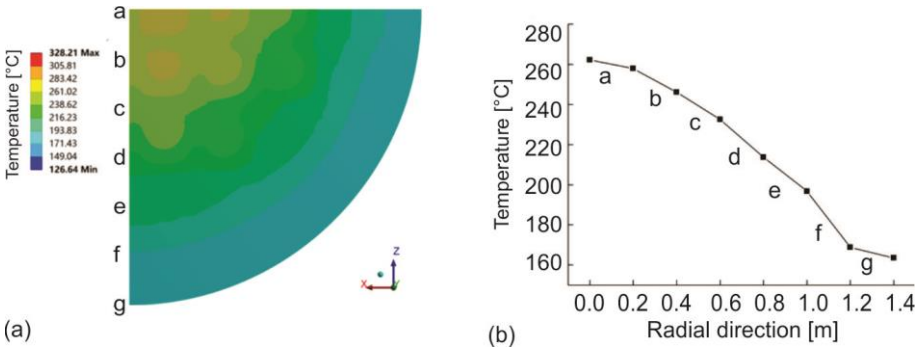

Figure 8. Temperature contours and curve of radial cross section at 2 m height; (a) temperature distribution cloud map (b) temperature curve

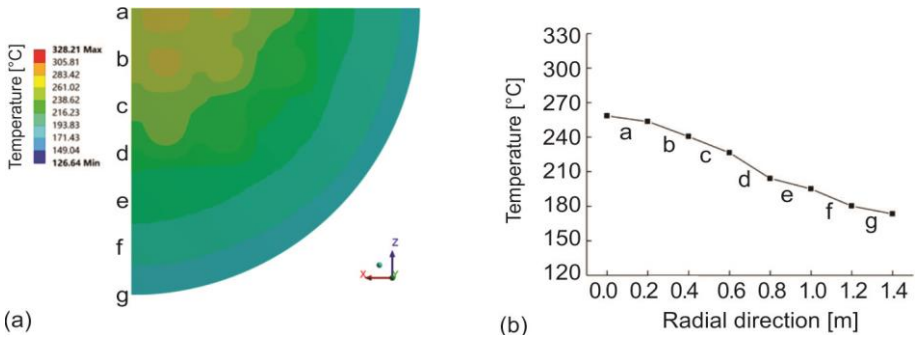

Figure 9. Temperature contours and curve of the radial cross section at 3 m height; (a) temperature distribution cloud map (b) temperature curve

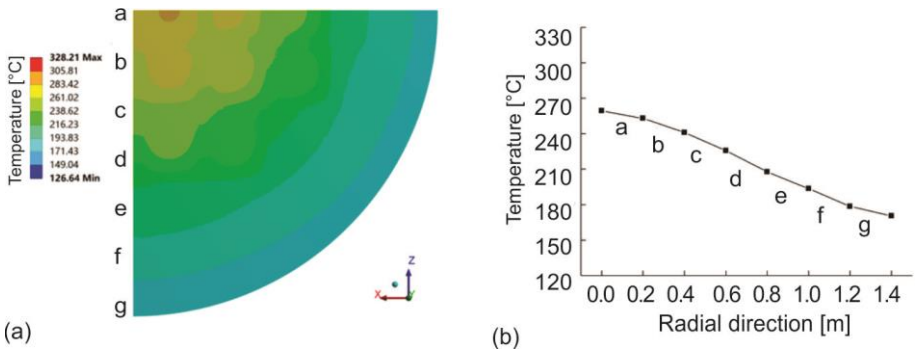

Figure 10. Temperature contours and curve of the radial cross section at 4 m height; (a) temperature distribution cloud map (b) temperature curve

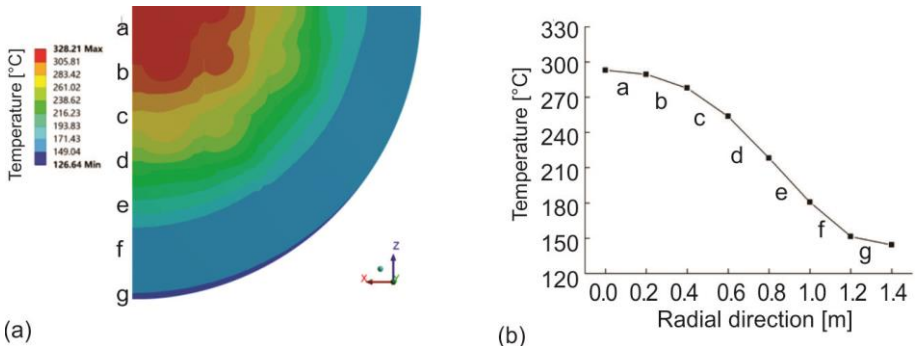

Figure 11. Temperature contours and curve of the radial cross section at 5 m height; (a) temperature distribution cloud map (b) temperature curve

Conclusions

According to the design parameters of AP1000, combined with the NAC-STC transport cask, the calculation model is established and simplified accordingly. The temperature field distribution of each part of the cask is studied by the thermal steady-state analysis module of ANSYS. The main conclusions are as follows.

- Under typical transportation environment with an ambient temperature of 22 ℃, the transport cask can transport the spent fuel assemblies with the decay heat power of 1.08 kW. The transport cask has good decaying heat extraction performance. Furthermore, the maximum temperature of the O-type sealing ring, the photon shielding layer and the neutron shielding layer are all lower than the safety limit of the corresponding material.
- Under normal transportation conditions, the spent fuel assembly located in the innermost part of the transport cask has the highest average temperature, and the highest temperature appears in the upper middle part. The highest temperature is 328 ℃, which is lower than the safety limit temperature 360 ℃ of the cladding.
- The temperature distribution of the cross-sections at different positions of the designed cask is consistent with the corresponding radial temperature distribution. The larger radial temperature distribution gradient near the heat transfer plate indicates that the designed heat transfer plate has a useful function of deriving decay heat, and the areas filled with helium also played a good heat transfer effect.

Acknowledgment

This work was supported by the Henan Province Key Specialized Research and Development Breakthrough Program in China (No. 192102210238) and the Scientific Research Project of High-Level Talents of North China University of Water Resources and Electric Power (No. 201705011).

References

[1] Wang, H., *et al*., Research Progress on Spent Fuel Transport Containers, *Mechanical Engineer*, (2015), 12, pp. 65-69
[2] Banerjee, K., Scaglione, J. M., *Criticality Safety Analysis of As-Loaded Spent Nuclear Fuel Casks*. Oak Ridge National Lab., Oak Ridge, Tenn., USA, 2015
[3] Saegusa, T., *et al*., Transport and Storage of Spent Nuclear Fuel, in: *Safe and Secure Transport and Storage of Radioactive Materials*, Woodhead Publishing, Sawston, UK, 2015, pp. 199-229
[4] Zinet, M., *et al*., Spent Fuel Transportation Cask Under Accidental Fire Conditions*:* Numerical Analysis of Gas Transport Phenomena Affecting Heat Transfer in Shielding Materials, *Progress in Nuclear Energy, 117* (2019), May, 103045
[5] Linnemann, K., *et al*., Considerations on Spent Fuel Behavior for Transport After Extended Storage. *Kerntechnik, 83* (2018), 6, pp. 488-494
[6] Herranz, L. E., *et al*. CFD Analysis of a Cask for Spent Fuel Dry Storage: Model fundamentals and sensitivity studies, *Annals of Nuclear Energy, 76* (2015), Feb., pp. 54-62
[7] Wix, S. D., Hohnstreiter. G. F., Convective Effects in a Regulatory and Proposed Fire Model. No. SAND-95-0207C; CONF-951203-49, Sandia National Labs., Albuquerque, N. Mex., USA, 1995
[8] Bullard, T., *et al*., Thermal Analysis of Proposed Transport Cask for Three Advanced Burner Reactor Used Fuel Assemblies, *Packaging, Transport, Storage & Security of Radioactive Material, 21* (2010), 3, pp. 158-164
[9] Frano, R. Lo., *et al*., Thermal Analysis of a Spent Fuel Cask in Different Transport Conditions, *Energy 36* (2011), 4, pp. 2285-2293
[10] Xu, P., *et al*., Research on AP1000 Spent Fuel Storage Facilities, *Nuclear Science and Engineering*, (2018), 04, pp.718-723
[11] Cao, B., *et al*., Preliminary Analysis of the Physical Characteristics of Typical Fuel Assemblies of AP1000, *Atomic Energy Science and Technology, 47* (2013), s2, pp. 599-602
[12] Schulz, T. L., Conway, L. E., Westinghouse AP1000 Containment Design, *Proceedings*, 13th International Conference on Nuclear Engineering Abstracts, Beijing, 2015
[13] Westinghouse, L. L. C., Westinghouse AP1000 Design Control Document Rev. 19. Westinghouse Electirc Company LLC, 2011
[14] Palacio, A., Design Process for Dual-Purpose Nuclear Spent Fuel Casks, *Energy Procedia, 127* (2017), Sept., pp. 398-406
[15] Lee, H. H., *Finite Element Simulations with ANSYS Workbench 18*, SDC Publications, Mission, Kans., USA, 2018
[16] Xu, Y., *et al*. Thermal Analysis on NAC-STC Spent Fuel Transport Cask Under Different Transport Conditions, *Nuclear Engineering and Design*, 265 (2013), Dec., pp.682-690
[17] Bahney, R. H., Lotz, T. L., Spent Nuclear Fuel Effective Thermal Conductivity Report. Prepared for the US DOE, Yucca Mountain Site Characterization Project Office by TRW Environmental Safety Systems, Inc., 1996
[18] Yang, S. M., Tao, W. Q., *Heat Transfer*, 4th ed., Higher Education Press, Beijing, China, 2006
[19] Jia, Z. Y., *Source Term Calculation Analysis and Research*, China Institute of Atomic Energy Science, 2004
[20] Weaver, D., Transportation and Storage of Radioactive Materials in the USA, *Security of Radioactive Material, 21* (2010), 4, pp. 186-188
[21] Hassen, A. A., Ahmed, K., Thermal Analysis of Concrete Cask in Normal and Cident Conditions, *Arab Journal of Nuclear Sciences and Applications, 50* (2017), 2, pp. 49-54

Paper submitted: October 23, 2019
Paper revised: November 19, 2019
Paper accepted: December 5, 2019